Journal of Sound and Vibration (2000) **234**(5), 841–858
doi:10.1006/jsvi.2000.2903, available online at http://www.idealibrary.com on IDEAL®

FREE-VIBRATION ANALYSIS OF RIGHT TRIANGULAR PLATES WITH VARIABLE THICKNESS

T. SAKIYAMA

Department of Structural Engineering, Nagasaki University, Nagasaki 852, *Japan*

AND

M. HUANG

Graduate School of Marine Science and Engineering, Nagasaki University, Nagasaki 852, *Japan*

(*Received* 17 *June* 1999, *and in final form* 18 *January* 2000)

An approximate method for analyzing the free vibration of right triangular plates with arbitrary variable thickness and various boundary conditions is proposed. In this paper, a right triangular plate is considered as a kind of rectangular plate with non-uniform thickness. Therefore, the free-vibration characteristics of any right triangular plate are obtained by analyzing the equivalent rectangular plate with non-uniform thickness. The approximate method is based on the Green function of an equivalent rectangular plate. The Green function of a rectangular plate with arbitrary variable thickness is obtained as a discrete-form solution for deflection of the plate with a concentrated load. By applying the Green function, the free-vibration problem of plate is translated into the eigenvalue problem of matrix.

1. INTRODUCTION

The determination of the free-vibration frequencies of right triangular plates is an important engineering problem. Thin right triangular plates with uniform thickness have been studied by many researchers. Gorman [1–3] exploited the superposition method for analyzing the problem of obtaining the eigenvalues and mode shapes for the right triangular plates with combinations of clamped–simply supported boundary conditions. Lam *et al.* [4] obtained the natural frequencies and mode shapes of triangular plates by applying the Rayleigh–Ritz method. Liew [5] analyzed the natural frequencies of triangular plates with curved internal supports. Liew and Lim [6] studied the transverse vibration of trapezoidal plates of variable thickness and showed the natural frequencies of triangular plates as a special case of trapezoidal plates. Saliba [7, 8] reported the modified superposition method to confirm the successful superposition principles and provided numerical data and mode shapes for right triangular plates with all possible combinations of clamped and simply supported boundary conditions. Kim and Dickinson [9] gave a straightforward and simple method by applying the Rayleigh–Ritz method for the free vibration of thin, right triangular plates which may have any combination of free, simply supported or clamped boundary conditions. For the right triangular plates with linearly varying thickness, Mirza and Bijlani [10] solved the problem of the natural frequencies and mode shapes of cantilevered triangular plates with linearly variable thickness by using the finite element

0022-460X/00/300841 + 18 $35.00/0

technique. As a special case of trapezoidal plates, Liew *et al.* [11] analyzed the free vibration of triangular plates with linearly varying thickness in one direction by the Rayleigh–Ritz method. Singh and Saxena [12] investigated a general triangular plate with the thickness varying linearly as a function of the co-ordinates in the plane of the plate. McGee and Giaimo [13] analyzed three-dimensional vibrations of cantilevered right triangular plates with moderate thickness. Kitipornchai *et al.* [14] investigated free vibration of isosceles triangular Mindlin plates. Liew *et al.* [15] analyzed three-dimensional vibrations of cantilevered right triangular plates as a case of skewed trapezoids.

In this paper, an approximate method for analyzing the free vibration of thin or moderately thick, right triangular plates with arbitrary variable thickness is proposed. A right triangular plate can be considered finally as a kind of rectangular plate with non-uniform thickness. Namely, a right triangular plate can be translated into a circumscribed rectangular plate whose additional part has the same thickness as that of the original part or extremely thin thickness compared with it and some intermediate point supports along the original diagonal edge according to its boundary condition. Therefore, the free-vibration characteristics of any right triangular plate are obtained by analyzing an equivalent rectangular plate with non-uniform thickness.

The approximate method is based on the Green function of an equivalent rectangular plate. The Green function of a rectangular plate with arbitrary variable thickness is obtained as a discrete-form solution [16] for deflection of the plate with a concentrated load. The discrete-form solution is obtained at each discrete point equally distributed on the plate. By applying the Green function, the free-vibration problem of plate is translated into the eigenvalue problem of matrix. The convergence and accuracy of the numerical solutions for the natural frequency parameter calculated by the proposed method are investigated, and the lowest eight frequency parameters and their modes of free vibration are shown for some right triangular plates.

2. DISCRETE GREEN FUNCTION OF RECTANGULAR PLATE WITH NON-UNIFORM THICKNESS AND POINT SUPPORTS

The Green function of a plate-bending problem is given by the displacement function of the plate with a unit concentrated load, so the Green function $w(x, y, x_q, y_r)/\bar{P}$ of rectangular plates can be obtained from the fundamental differential equations of rectangular plate with a concentrated load $\bar{P}$ at a point (x_q, y_r), non-uniform thickness and point supports at each discrete point (x_c, y_d) shown in Figure 1, which are given by the following equations:

$$\frac{\partial Q_x}{\partial x} + \frac{\partial Q_y}{\partial y} + \sum_{c=0}^{m}\sum_{d=0}^{n} \bar{P}_{1cd}\delta(x - x_c)\delta(y - y_d) + \bar{P}\delta(x - x_q)\delta(y - y_r) = 0, \tag{1a}$$

$$\frac{\partial M_y}{\partial y} + \frac{\partial M_{xy}}{\partial x} - Q_y + \sum_{c=0}^{m}\sum_{d=0}^{n} \bar{P}_{2cd}\delta(x - x_c)\delta(y - y_d) = 0, \tag{1b}$$

$$\frac{\partial M_x}{\partial x} + \frac{\partial M_{xy}}{\partial y} - Q_x - \sum_{c=0}^{m}\sum_{d=0}^{n} \bar{P}_{3cd}\delta(x - x_c)\delta(y - y_d) = 0, \tag{1c}$$

$$\frac{\partial \theta_x}{\partial x} + \nu\frac{\partial \theta_y}{\partial y} = \frac{M_x}{D}, \qquad \frac{\partial \theta_y}{\partial y} + \nu\frac{\partial \theta_x}{\partial x} = \frac{M_y}{D}, \tag{1d,e}$$

$$\frac{\partial \theta_x}{\partial y} + \frac{\partial \theta_y}{\partial x} = \frac{2}{(1-\nu)}\frac{M_{xy}}{D}, \qquad \frac{\partial w}{\partial x} + \theta_x = \frac{Q_x}{Gt_s}, \qquad \frac{\partial w}{\partial y} + \theta_y = \frac{Q_y}{Gt_s}, \tag{1f–h}$$

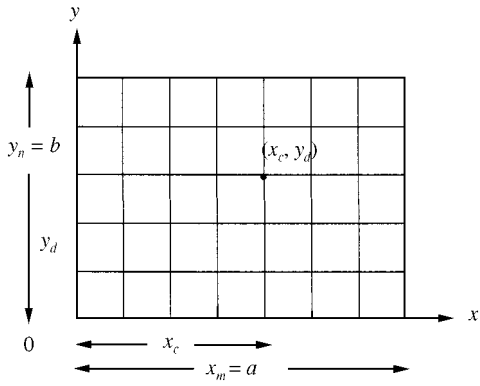

Figure 1. Position of point support.

where Q_x, Q_y are the shearing forces, M_{xy} is the twisting moment, M_x, M_y are the bending moments, θ_x, θ_y are the slopes, w is the deflection, $D = Eh^3/12(1-\nu^2)$ the bending rigidity, E, G the modulus, shear modulus of elasticity, ν the Poisson ratio, $h = h(x, y)$ the thickness of the plate, $t_s = h/1{\cdot}2$, $\bar{P}_{1cd}$ the vertical reaction, $\bar{P}_{2cd}$, $\bar{P}_{3cd}$ the moment reactions around the x- and y-axis and $\delta(x - x_c)$, $\delta(y - y_d)$ are the Dirac's delta functions.

By introducing the following non-dimensional expressions,

$$[X_1, X_2] = \frac{a^2}{D_0(1-\nu^2)}[Q_y, Q_x], \qquad [X_3, X_4, X_5] = \frac{a}{D_0(1-\nu^2)}[M_{xy}, M_y, M_x],$$

$$[X_6, X_7, X_8] = [\theta_y, \theta_x, w/a],$$

the differential equations (1a)–(1h) are rearranged together as follows:

$$\sum_{e=1}^{8}\left[F_{1te}\frac{\partial X_e}{\partial \zeta} + F_{2te}\frac{\partial X_e}{\partial \eta} + F_{3te}X_e\right] + \sum_{f=1}^{3}\sum_{c=0}^{m}\sum_{d=0}^{n} P_{fcd}\delta(\eta - \eta_c)\delta(\zeta - \zeta_d)\delta_{ft}$$

$$+ P\delta(\eta - \eta_q)\delta(\zeta - \zeta_r)\delta_{1t} = 0, \tag{2}$$

where $t = 1$–8, $\mu = b/a$, $\eta = x/a$, $\zeta = y/b$, $D_0 = Eh_0^3/12(1-\nu^2)$ is the standard bending rigidity, h_0 the standard thickness of a plate, a, b the breadth, length of a rectangular plate, $[P, P_{1cd}, P_{2cd}, P_{3cd}] = [\bar{P}a, \bar{P}_{1cd}a, \bar{P}_{2cd}, -\bar{P}_{3cd}]/D_0(1-\nu^2)$ δ_{ft} the Kronecker's delta, and F_{1te}, F_{2te}, F_{3te} are defined in Appendix A.

3. DISCRETE SOLUTION OF FUNDAMENTAL DIFFERENTIAL EQUATION

By applying the method used in reference [16], with a rectangular plate divided vertically into m equal-length parts and horizontally into n equal-length parts as shown in Figure 2, the plate can be considered as a group of discrete points which are the intersections of the $(m+1)$-vertical and $(n+1)$-horizontal dividing lines. In this paper, the rectangular area, $0 \leqslant \eta \leqslant \eta_i$, $0 \leqslant \zeta \leqslant \zeta_j$, corresponding to the arbitrary intersection (i, j) as shown in Figure 2 is denoted as the area $[i, j]$, the intersection (i, j) denoted by ● is called the main point of the area $[i, j]$, the intersections denoted by ○ are called the inner-dependent points of the

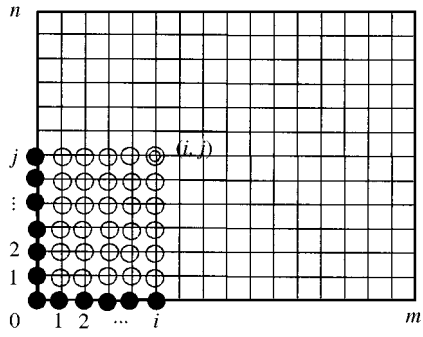

Figure 2. Discrete points on plate.

area, and the intersections denoted by ● are called the boundary-dependent points of the area.

By integrating equation (2) over the area $[i, j]$, the following integral equation is obtained:

$$\sum_{e=1}^{8}\left\{\begin{aligned}&F_{1te}\int_0^{\eta_i}[X_e(\eta,\zeta_j)-X_e(\eta,0)]\,\mathrm{d}\eta+F_{2te}\int_0^{\zeta_j}[X_e(\eta_i,\zeta)-X_e(0,\zeta)]\,\mathrm{d}\zeta\\&+F_{3te}\int_0^{\eta_i}\int_0^{\zeta_f}X_e(\eta,\zeta)\,\mathrm{d}\eta\,\mathrm{d}\zeta\end{aligned}\right\}$$

$$+\sum_{f=1}^{3}\sum_{c=0}^{m}\sum_{d=0}^{n}P_{fcd}u(\eta-\eta_c)u(\zeta-\zeta_d)\delta_{ft}+Pu(\eta-\eta_q)u(\zeta-\zeta_r)\delta_{1t}=0, \tag{3}$$

where

$$u(\eta_i-\eta_c)=0(i<c),0{\cdot}5(i=c),1(i>c),\qquad u(\zeta_j-\zeta_d)=0(j<d),0{\cdot}5(j=d),1(j>d).$$

Next, by applying the numerical integration method the simultaneous equation for the unknown quantities $X_{eij}=X_e(\eta_i,\zeta_j)$ at the main point, (i, j) of the area $[i, j]$ is obtained as follows:

$$\sum_{e=1}^{8}\left\{F_{1te}\sum_{k=0}^{i}\beta_{ik}(X_{ekj}-X_{ek0})+F_{2te}\sum_{l=0}^{i}\beta_{jl}(X_{eil}-X_{e0l})+F_{3te}\sum_{k=0}^{i}\sum_{l=0}^{j}\beta_{ik}\beta_{jl}X_{ekl}\right\}$$

$$+\sum_{f=1}^{3}\sum_{c=0}^{m}\sum_{d=0}^{n}P_{fcd}u_{ic}u_{jd}\delta_{ft}+Pu_{1q}u_{jr}\delta_{1t}=0, \tag{4}$$

where

$$u_{ic}=\begin{cases}0 & (i<c),\\0{\cdot}5 & (i=c),\\1 & (i>c),\end{cases}\qquad u_{jd}=\begin{cases}0 & (j<d),\\0{\cdot}5 & (j=d),\\1 & (j>d),\end{cases}\qquad \alpha_{ik}=\begin{cases}0{\cdot}5 & (k=0,i),\\1 & (k\neq 0,i),\end{cases}\qquad \alpha_{jl}=\begin{cases}0{\cdot}5 & (l=0,j),\\1 & (l\neq 0,j),\end{cases}$$

$$\beta_{ik}=\alpha_{ik}/m,\qquad \beta_{jl}=\alpha_{jl}/n.$$

The solution X_{pij} of the simultaneous equation (4) is obtained as follows:

$$X_{pij} = \sum_{e=1}^{8} \left\{ \begin{array}{l} \sum_{k=0}^{i} \beta_{ik} A_{pe} [X_{ek0} - X_{ekj}(1 - \delta_{ki})] + \sum_{l=0}^{j} \beta_{jl} B_{pe} [X_{e0l} - X_{eil}(1 - \delta_{lj})] \\ + \sum_{k=0}^{i} \sum_{l=0}^{j} \beta_{ik} \beta_{jl} C_{pekl} X_{ekl} (1 - \delta_{ki} \delta_{lj}) \end{array} \right\}$$

$$- \sum_{f=1}^{3} \gamma_{pf} \sum_{c=0}^{m} \sum_{d=0}^{n} P_{fcd} u_{ic} u_{jd} - \gamma_{p1} P u_{iq} u_{jr}, \tag{5}$$

where $p = 1, 2, \ldots, 8$, $i = 1, 2, \ldots, m$, $j = 1, 2, \ldots, n$, and A_{pe}, B_{pe}, C_{pekl}, γ_{pf} are defined in Appendix B.

In equation (5), the quantity X_{pij} at the main point (i, j) of the area $[i, j]$ is related to the quantities X_{ek0} and X_{e0l} at the boundary-dependent points of the area and the quantities X_{ekj}, X_{eil} and X_{ekl} at the inner dependent points of the area. With the spreading of the area $[i, j]$ according to the regular order as $[1, 1], [1, 2], \ldots, [1, n], [2, 1], [2, 2], \ldots, [2, n], \ldots, [m, 1], [m, 2], \ldots, [m, n]$, a main point of smaller area becomes one of the inner-dependent points of the following larger areas. Whenever the quantity X_{pij} at the main point (i, j) is obtained by using equation (5) in the above-mentioned order, the quantities X_{ekj}, X_{eil} and X_{ekl} at the inner-dependent points of the following larger areas can be eliminated by substituting the obtained results into the corresponding terms on the right-hand side of equation (5). By repeating this process, the equation X_{pij} at the main point is related to only the quantities X_{vk0} $(v = 1, 3, 4, 6, 7, 8)$ and X_{s0l} $(s = 2, 3, 5, 6, 7, 8)$ which are six independent quantities at each boundary-dependent point along the horizontal axis and the vertical axis in Figure 2 respectively. The result is as follows:

$$X_{pij} = \sum_{k=0}^{i} \left\{ \begin{array}{l} a_{1pijk1}(Q_y)_{k0} + a_{1pijk2}(M_{xy})_{k0} + a_{1pijk3}(M_y)_{k0} \\ + a_{1pijk4}(\theta_y)_{k0} + a_{1pijk5}(\theta_x)_{k0} + a_{1pijk6}(w)_{k0} \end{array} \right\}$$

$$+ \sum_{l=0}^{j} \left\{ \begin{array}{l} a_{2pijl1}(Q_x)_{0l} + a_{2pijl2}(M_{xy})_{0l} + a_{2pijl3}(M_x)_{0l} \\ + a_{2pijl4}(\theta_y)_{0l} + a_{2pijl5}(\theta_x)_{0l} + a_{2pijl6}(w)_{0l} \end{array} \right\}$$

$$+ \sum_{f=1}^{3} \sum_{c=0}^{m} \sum_{d=0}^{n} q_{fpijcd} P_{fcd} + \bar{q}_{pij} P, \tag{6}$$

where $(Q_y) = X_1$, $(Q_x) = X_2$, $(M_{xy}) = X_3$, $(M_y) = X_4$, $(M_x) = X_5$, $(\theta_y) = X_6$, $(\theta_x) = X_7$, $(w) = X_8$, and a_{hpijuv}, q_{fpijcd}, $\bar{q}_{fpij}$ are defined in Appendix C.

Equation (6) gives the discrete solution of the fundamental differential equation (2) of plate-bending problem, and the discrete Green function of a plate is obtained from $X_{8ij} = G(x_i, y_j, x_q, y_r) \cdot [\bar{P}a/D_0(1 - \nu^2)]$ which is the displacement at the point (x_i, y_j) of a plate with a concentrated load $\bar{P}$ at a point (x_q, y_r).

4. INTEGRAL CONSTANT AND BOUNDARY CONDITION OF RECTANGULAR PLATE

The integral constants $(Q_y)_{k0}, (M_{xy})_{k0}, \ldots, (w)_{k0}, (Q_x)_{0l}, (M_{xy})_{0l}, \ldots, (w)_{0l}$ being involved in the discrete solution (6) are to be evaluated by the boundary conditions of a rectangular

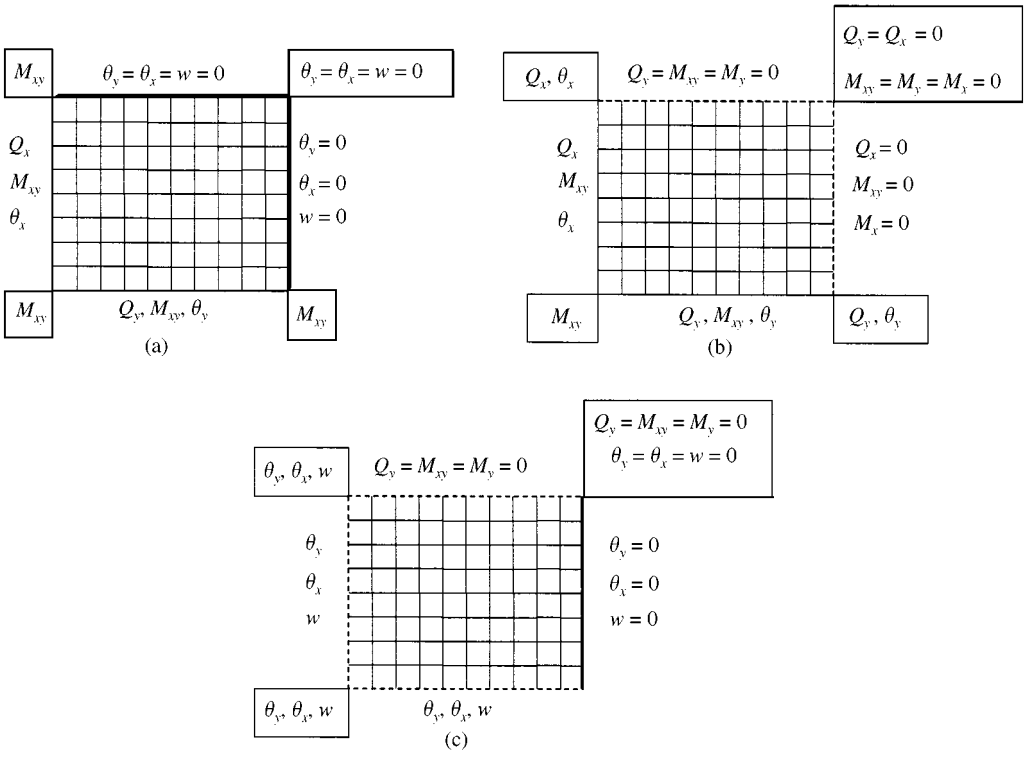

Figure 3. (a) Plate with simple edges and fixed edges. (b) Plate with simple edges and free edges. (c) Cantilever plate.

plate. The combinations of the integral constants and the boundary conditions for some cases are shown in Figures 3(a)–3(c), in which the integral constants and the boundary conditions at the four corners are shown in the boxes. The integral constants and the boundary conditions along the four edges are given at each of the equally spaced discrete points. In this paper, simply supported, fixed and free edges are denoted by solid line (——), thick solid line (▬▬) and dotted line (- - - - -) respectively.

5. EQUIVALENT RECTANGULAR PLATE OF RIGHT TRIANGULAR PLATE

A right triangular plate is different from a rectangular plate, but it is considered as a kind of rectangular plate by translating into a circumscribed equivalent rectangular plate with non-uniform thickness and intermediate point supports, whose additional part is considered theoretically to have the same thickness as that of the original part or extremely thin thickness compared with the original part according to the boundary condition of the diagonal edge of the original plate.

The thickness of the actual part of the original right triangular plate is expressed by h_0, and the thickness of the additional part of each equivalent rectangular plate is expressed by h in this paper.

Typical translations from some original right triangular plates to their equivalent rectangular plates are shown in Figure 4. In Figure 4, a fixed diagonal edge of the original

plate is translated into a line with some equally arranged point supports shown by the thick dotted line (·····) and an additional equally thick part with two fixed edges. The values of three reactions P_{1cd}, P_{2cd}, P_{3cd} at each point support of the equivalent plate are determined by the following three conditions:

$$\theta_t = \theta_t \sin\alpha + \theta_y \cos\alpha = 0, \qquad \theta_n = \theta_x \cos\alpha - \theta_y \sin\alpha = 0, \qquad w = 0,$$

where

$$\alpha = \tan^{-1}(b/a).$$

The first condition means that the slope around the tangential axis of the line of point supports is zero at each point support. The second condition means that the slope around the normal axis of the line of point supports is zero, and the third condition means zero deflection at each point support. In Figure 4, a simply supported diagonal edge of the original plate is translated into a line with some equally arranged point supports shown by the thick dotted line (·····) and an additional extremely thin part with two free edges. In this case the values of three reactions P_{1cd}, P_{2cd}, P_{3cd} at each point support of the equivalent plate are determined by the following three conditions:

$$M_t = M_x \sin^2\alpha + M_y \cos^2\alpha + 2M_{xy} \sin\alpha \cos\alpha = 0, \qquad \theta_n = 0, \qquad w = 0.$$

The first condition means that the bending moment around the tangential axis of the line of point supports is zero at each point support. The second condition means that the slope around the normal axis of the line of point supports is zero, and the third condition means zero deflection at each point support. In Figure 4, a free diagonal edge of the original plate is translated into an additional extremely thin part with two free edges.

In the free-vibration analysis of the equivalent rectangular plates for each right triangular plate, the mass of the additional triangular part is treated as equal to zero.

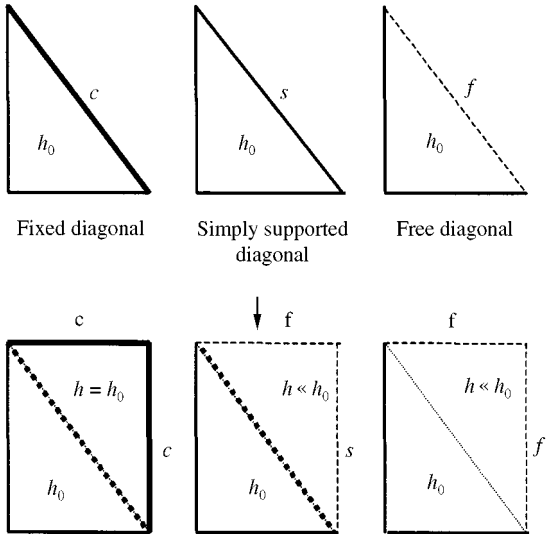

Figure 4. Triangular plates and their equivalent rectangular plates.

6. CHARACTERISTIC EQUATION OF FREE VIBRATION OF RECTANGULAR PLATE WITH NON-UNIFORM THICKNESS AND POINT SUPPORTS

By applying the Green function $w(x_0, y_0, x, y)/\bar{P}$ which is the displacement at a point (x_0, y_0) of a plate with a concentrated load $\bar{P}$ at a point (x, y), the displacement amplitude $\hat{w}(x_0, y_0)$ at a point (x_0, y_0) of the equivalent rectangular plate during the free vibration is given as follows:

$$\hat{w}(x_0, y_0) = \int_0^b \int_0^a \rho h \omega^2 \hat{w}(x, y)[w(x_0, y_0, x, y)/\bar{P}]\, \mathrm{d}x\, \mathrm{d}y, \tag{7}$$

where ρ is the mass density of the plate material.

By using the non-dimensional expressions,

$$\lambda^4 = \frac{\rho_0 h_0 \omega^2 a^4}{D_0(1-\nu^2)}, \qquad H(\eta, \zeta) = \frac{\rho(x, y)}{\rho_0}\frac{h(x, y)}{h_0}, \qquad W(\eta, \zeta) = \frac{\hat{w}(x, y)}{a},$$

$$G(\eta_0, \zeta_0, \eta, \zeta) = \frac{w(x_0, y_0, x, y)}{a}\frac{D_0(1-\nu^2)}{\bar{P}a},$$

where ρ_0 is the standard mass density the integral equation (7) can be rewritten as follows:

$$W(\eta_0, \zeta_0) = \int_0^1 \int_0^1 \mu\lambda^4 H(\eta, \zeta) G(\eta_0, \zeta_0, \eta, \zeta) W(\eta, \zeta)\, \mathrm{d}\eta\, \mathrm{d}\zeta. \tag{8}$$

By applying the numerical integration method mentioned in Section 3, equation (8) is discretely expressed as

$$\kappa W_{kl} = \sum_{i=0}^{m}\sum_{j=0}^{n} \beta_{mi}\beta_{nj} H_{ij} G_{klij} W_{ij}, \qquad \kappa = 1/(\mu\lambda^4). \tag{9}$$

From equation (9) homogeneous linear equations in $(m+1)\times(n+1)$ unknowns W_{00}, $W_{01}, \ldots, W_{0n}$, W_{10}, $W_{11}, \ldots, W_{1n}$, $\sim$, W_{m0}, $W_{m1}, \ldots, W_{mn}$ are obtained as follows:

$$\sum_{i=0}^{m}\sum_{j=0}^{n} (\beta_{mi}\beta_{nj} H_{ij} G_{klij} - \kappa\delta_{ik}\delta_{jl}) W_{ij} = 0 \qquad (k = 0, 1, \ldots, m, \qquad l = 0, 1, \ldots, n). \tag{10}$$

The characteristic equation of the free vibration of the equivalent rectangular plate is obtained from equation (10) as follows:

$$\begin{vmatrix} \mathbf{K}_{00} & \mathbf{K}_{01} & \mathbf{K}_{02} & \cdots & \mathbf{K}_{0m} \\ \mathbf{K}_{10} & \mathbf{K}_{11} & \mathbf{K}_{12} & \cdots & \mathbf{K}_{1m} \\ \mathbf{K}_{20} & \mathbf{K}_{21} & \mathbf{K}_{22} & \cdots & \mathbf{K}_{2m} \\ & \cdots & \cdots & & \\ \mathbf{K}_{m0} & \mathbf{K}_{m1} & \mathbf{K}_{m2} & \cdots & \mathbf{K}_{mm} \end{vmatrix} = 0, \tag{11}$$

where

$$\mathbf{K}_{ij}=\beta_{mj}\begin{bmatrix}\beta_{n0}H_{j0}G_{i0j0}-\kappa\delta_{ij} & \beta_{n1}H_{j1}G_{i0j1} & \beta_{n2}H_{j2}G_{i0j2} & \cdots & \beta_{nn}H_{jn}G_{i0jn}\\ \beta_{n0}H_{j0}G_{i1j0} & \beta_{n1}H_{j1}G_{i1j1}-\kappa\delta_{ij} & \beta_{n2}H_{j2}G_{i1j2} & \cdots & \beta_{nn}H_{jn}G_{i1jn}\\ \beta_{n0}H_{j0}G_{i2j0} & \beta_{n1}H_{j1}G_{i2j1} & \beta_{n2}H_{j2}G_{i2j2}-\kappa\delta_{ij} & \cdots & \beta_{nn}H_{jn}G_{i2jn}\\ & \cdots & \cdots & & \\ \beta_{n0}H_{j0}G_{inj0} & \beta_{n1}H_{j1}G_{inj1} & \beta_{n2}H_{j2}G_{inj2} & \cdots & \beta_{nn}H_{jn}G_{injn}-\kappa\delta_{ij}\end{bmatrix}.$$

7. NUMERICAL WORK

Numerical solutions for the natural frequency parameter λ and the mode have been investigated for some thin, non-uniform or moderately thick triangular plates. The convergent values for the natural frequency parameter λ have been obtained by using Richardson's extrapolation formula for two case of combinations of numbers of division m and n. In all the tables and figures, the symbols s, c and f denote simply supported, clamped and free edges, respectively, the first indicating the conditions at $y = 0$ ($\zeta = 0$), the second at the hypotenuse and the third at $x = 0$ ($\eta = 0$). In this paper, the numerical results are shown within three cases of boundary conditions scs, sss and cff.

7.1. CONVERGENCE AND ACCURACY OF NUMERICAL RESULTS FOR RIGHT TRIANGULAR PLATES WITH UNIFORM OR LINEARLY VARYING THICKNESS

In order to examine the convergence of numerical values for the natural frequency parameter λ obtained from the proposed method and determine the suitable values of the thickness ratio h/h_0 of the extremely thin part thickness h and the actual part thickness h_0 and the numbers of division m and n, the lowest eight natural frequency parameters for three or two cases of right triangular plates shown in Figure 5 were analyzed. In this case, these plates have uniform thickness and an aspect ratio $b/a = 1$. The results are shown in Figures 6(a)–6(c), 7(a) and 7(b). These show a good convergence of numerical solutions by the proposed method. After studying the curves of Figures 6(a)–6(c), 7(a) and 7(b), it seems actually sufficient to set the thickness ratio $h/h_0 < \frac{1}{4}$ for the right triangular plate with simply supported or free diagonal edge and the number of division $m(=n) > 12$ for scs right triangular plates and $m(=n) > 10$ for sss and cff right triangular plates.

In order to demonstrate the accuracy of numerical results for the natural frequency parameter λ obtained from the proposed method, the lowest eight natural frequency parameters for the four right triangular plates with two aspects ratios, $b/a = 1$ and 1·5 are presented in Tables 1(a)–(c) and compared with previously published results by Kim and

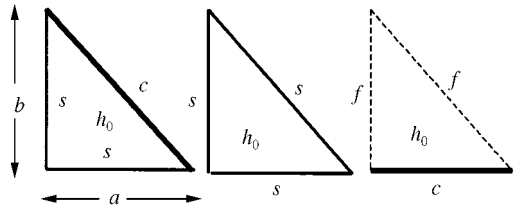

Figure 5. Right triangular plates with various boundary conditions.

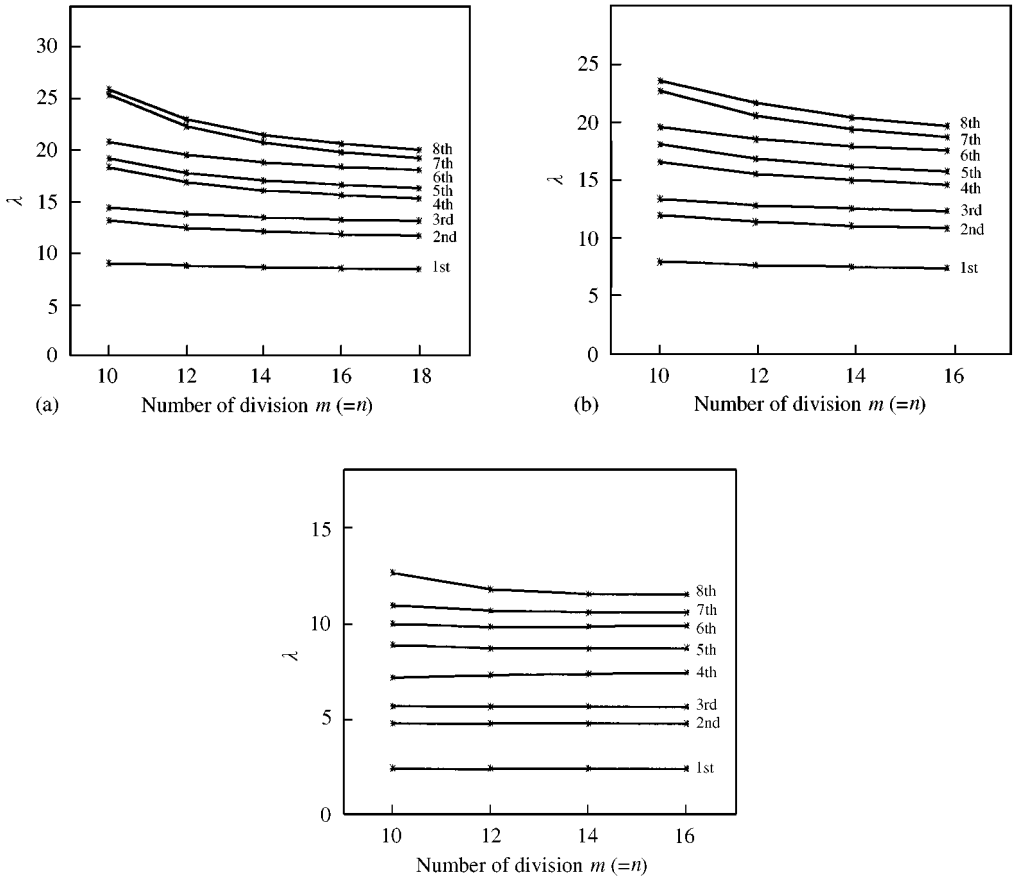

Figure 6. (a) Convergence of natural frequency parameter λ of scs isosceles right triangular plate $h = h_0$; (b) Convergence of natural frequency parameter λ of sss isosceles right triangular plate $h = h_0/5$; (c) Convergence of natural frequency parameter λ of cff isosceles right triangular plate $h = h_0/5$.

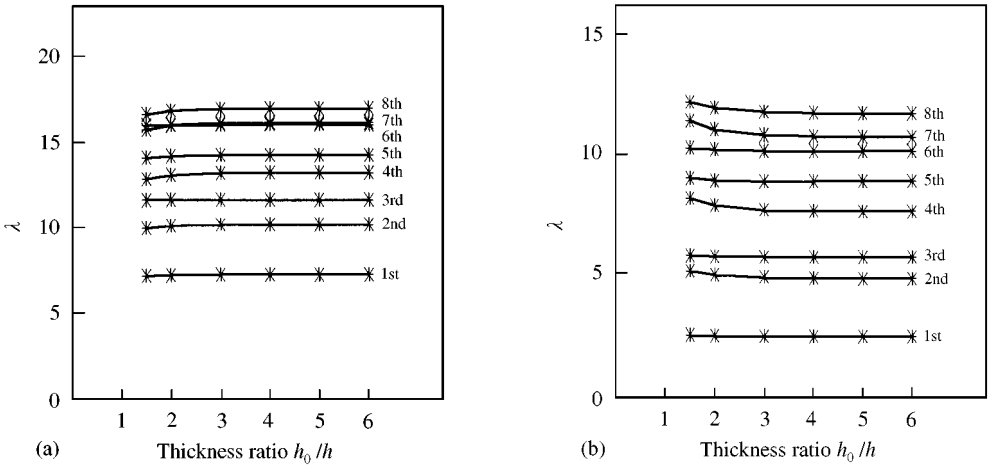

Figure 7. (a) Convergence of natural frequency parameter of sss right triangular plate with uniform thickness $b/a = 1$, $m = 14, 16$; (b) Convergence of natural frequency parameter of cff right triangular platewith uniform thickness $b/a = 1$, $m = 14, 16$.

TABLE 1(a)

Natural frequency parameters λ for scs right triangular plates

	$b/a = 1$, uniform				$b/a = 1{\cdot}5$, uniform			
	m				m			
Mode	16	16	Extra-polation	Reference [9]	16	18	Extra-polation	Reference [9]
1	8·602	8·548	8·343	8·305	7·196	7·149	6·973	6·940
2	11·945	11·804	11·272	11·267	9·785	9·669	9·233	9·230
3	13·374	13·246	12·766	12·726	11·356	11·238	10·796	10·768
4	15·697	15·396	14·261	14·378	12·598	12·365	11·486	11·556
5	16·758	16·483	15·446	15·575	14·177	13·924	12·973	13·080
6	18·492	18·220	17·198	17·288	15·616	15·227	13·762	13·915
7	19·902	19·334	17·193	—	15·828	15·547	14·489	—
8	20·709	20·176	18·170	—	17·363	16·898	15·146	—

TABLE 1(b)

Natural frequency parameters λ for sss right triangular plates

	$b/a = 1$, variable				$b/a = 1{\cdot}5$, uniform			
	m				m			
Mode	14	16	Extra-polation	Reference [11]	14	16	Extra-polation	Reference [9]
1	6·914	6·826	6·539	6·592	6·291	6·211	5·952	5·995
2	9·923	9·705	8·992	9·162	8·981	8·793	8·180	8·298
3	11·405	11·229	10·652	10·693	10·492	10·312	9·726	9·820
4	13·187	12·881	11·882	11·887	11·855	11·525	10·447	10·640
5	14·590	14·149	12·709	13·074	13·397	13·071	12·007	12·153
6	16·303	15·918	14·662	14·623	14·929	14·478	13·008	13·028
7	16·763	16·327	14·905	14·830	15·134	14·693	13·254	—
8	18·155	17·565	15·641	15·746	16·614	16·069	14·289	—

TABLE 1(c)

Natural frequency parameters λ for cff right triangular plates

	$b/a = 1$, variable				$b/a = 1{\cdot}5$, uniform			
	m				m			
Mode	14	16	Extra-polation	Reference [11]	14	16	Extra-polation	Reference [9]
1	2·714	2·722	2·748	2·763	1·682	1·687	1·705	1·736
2	4·193	4·196	4·205	4·217	3·488	3·492	3·506	3·563
3	4·889	4·908	4·917	5·048	4·190	4·204	4·250	4·322
4	5·768	5·765	5·756	5·729	5·505	5·506	5·509	5·576
5	6·617	6·584	6·476	6·598	6·522	6·537	6·588	6·695
6	7·504	7·470	7·361	7·353	7·656	7·632	7·555	7·660
7	8·027	7·973	7·793	7·894	8·289	8·270	8·210	—
8	8·883	8·848	8·733	8·775	9·071	9·041	8·941	—

Dickinson [9] for the uniform thickness plates and by Liew *et al.* [11] for the linearly varying thickness plates. The thickness ratio h_0/a of these plates is 0·01. In these examples, the scs plate and the sss and cff plates with the aspect ratio $b/a = 1{\cdot}5$ have uniform thickness and the sss and cff plates with the aspect ratio $b/a = 1$ have linearly varying thickness, and the thickness variation of the triangular plates is as follows:

$$\text{sss plate:} \quad h(\eta, \zeta) = h_0(1 - 0{\cdot}5\zeta), \qquad \text{cff plate:} \quad h(\eta, \zeta) = h_0(1 - \zeta).$$

Tables 1(a)–1(c) show that a close agreement is achieved. In Figures 8(a)–8(c) the corresponding nodal patterns are presented, and these are also confirmed to agree with the nodal patterns given in references [9, 11].

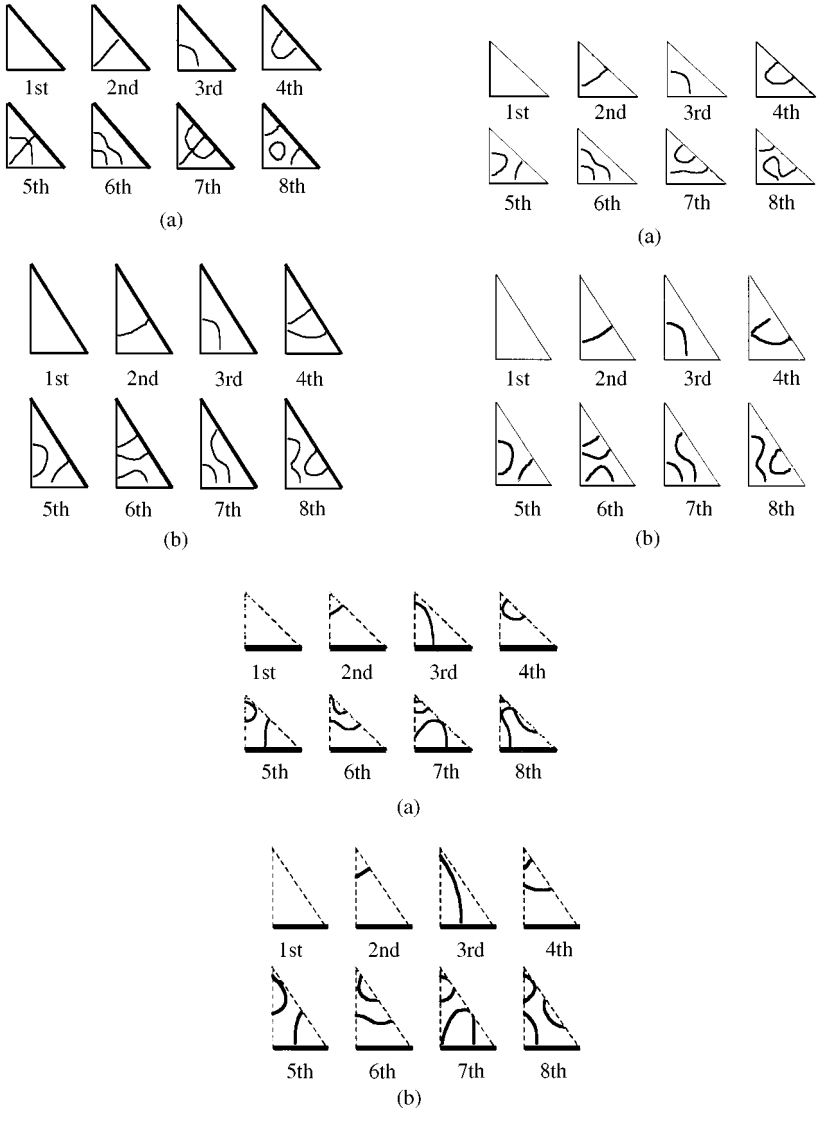

Figure 8. (a) Nodal patterns for scs right triangular plate: (a) $a/b = 1$; (b) $b/a = 1{\cdot}5$. (b) Nodal patterns for sss right triangular plate: (a) $a/b = 1$; (b) $b/a = 1{\cdot}5$. (c) Nodal patterns for cff right triangular plate: (a) $a/b = 1$; (b) $b/a = 1{\cdot}5$.

7.2. NUMERICAL RESULTS FOR RIGHT TRIANGULAR PLATES WITH VARIABLE THICKNESS

Numerical solutions for the lowest eight values of natural frequency parameter λ of scs and cff right triangular plates with two aspects ratios, $b/a = 1$ and 1·5 were analyzed. The thickness variation of each right triangular plate is as follows:

$$\text{scs plate:} \quad h(\eta, \zeta) = h_0[1 + \sin 0{\cdot}5\pi(\eta + \zeta)],$$

$$\text{cff plate:} \quad h(\eta, \zeta) = h_0[(1 - 0{\cdot}5(\eta^2 + \zeta^2)).$$

The thickness ratio h_0/a of these plates is 0·01. The results are presented in Tables 2(a) and 2(b). The corresponding nodal patterns are presented in Figures 9(a) and 9(b).

7.3. NUMERICAL RESULTS FOR RIGHT TRIANGULAR PLATES WITH MODERATE THICKNESS

Numerical solutions for the lowest eight values of natural frequency parameter λ and the corresponding nodal patterns of cff moderately thick right triangular plates with uniform

TABLE 2(a)

Natural frequency parameters λ for scs right triangular plates with variable thickness

	$b/a = 1$			$b/a = 1{\cdot}5$		
	m			m		
Mode	16	18	Extra-polation	16	18	Extra-polation
1	11·340	11·272	11·014	9·486	9·440	9·269
2	15·920	15·756	15·139	13·016	12·880	12·371
3	17·268	17·126	16·593	14·750	14·590	13·988
4	20·818	20·468	19·151	16·665	16·390	15·357
5	21·953	21·631	20·420	18·729	18·435	17·328
6	23·634	23·288	21·985	20·582	20·077	18·178
7	26·181	25·536	23·105	20·176	19·919	18·953
8	26·982	26·389	24·156	22·957	22·407	20·336

TABLE 2(b)

Natural frequency parameters λ for cff right triangular plates with variable thickness

	$b/a = 1$			$b/a = 1{\cdot}5$		
	m			m		
Mode	14	16	Extra-polation	14	16	Extra-polation
1	2·479	2·487	2·513	1·673	1·679	1·699
2	4·504	4·514	4·545	3·243	3·249	3·270
3	5·459	5·473	5·520	3·978	3·992	4·037
4	6·724	6·767	6·908	4·990	4·992	4·997
5	7·885	7·933	8·092	5·913	5·929	5·980
6	9·051	9·075	9·154	6·924	6·912	6·870
7	9·787	9·749	9·623	7·430	7·414	7·363
8	10·357	10·331	10·248	8·353	8·333	8·268

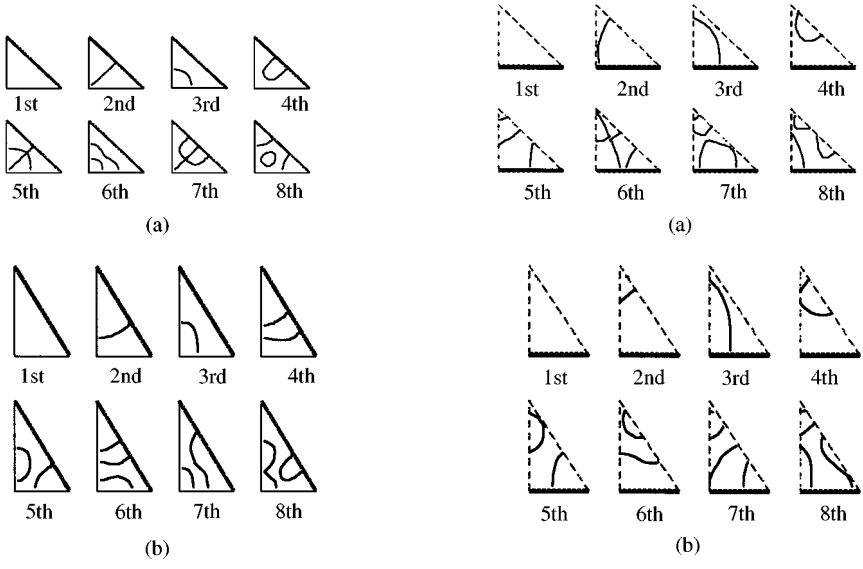

Figure 9. (a) Nodal patterns for scs right triangular plate with variable thickness: (a) $a/b = 1$; (b) $b/a = 1{\cdot}5$. (b) Nodal patterns for cff right triangular plate with variable thickness: (a) $a/b = 1$; (b) $b/a = 1{\cdot}5$.

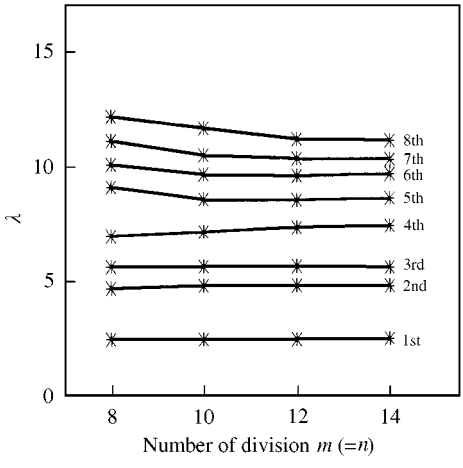

Figure 10. Convergence of natural frequency parameter λ of cff moderately thick uniform right triangular plate $h_0/a = 0{\cdot}061$, $h_0/h = 10$ ($b/a = 1$).

and variable thickness were analyzed. The aspect ratio b/a is equal to 1, and the thickness ratio h_0/a is equal to 0·061. The thickness variation of the right triangular plate with variable thickness is as follows:

$$\text{cff plate:} \quad h(\eta, \zeta) = h_0(1 - 0{\cdot}4\zeta).$$

The results for the convergence, nodal pattern and natural frequency are shown in Figures 10, 11 and Table 3 respectively. Figure 10 shows a good convergence of numerical solutions

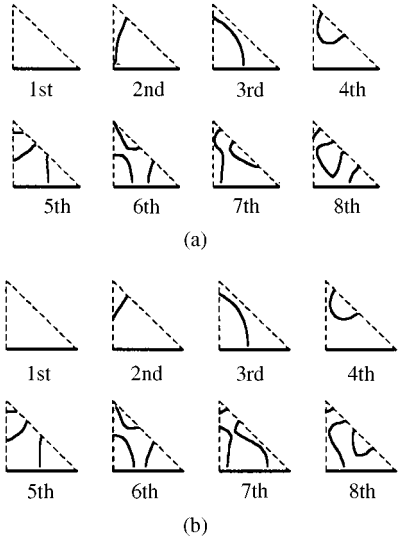

Figure 11. Nodal patterns for cff right triangular plates with moderate thickness: (a) uniform; (b) variable.

TABLE 3

Natural frequency parameters λ for cff moderately thick right triangular plates

	Uniform				Variable			
	m				*m*			
Mode	12	14	Extra-polation	Reference [13]	12	14	Extra-polation	Reference [13]
1	2·438	2·471	2·563	2·541	2·473	2·482	2·506	2·569
2	4·775	4·778	4·788	4·964	4·543	4·554	4·583	4·713
3	5·626	5·589	5·488	5·871	5·343	5.359	5·402	5·580
4	7·315	7·396	7·621	7·689	6·749	6·826	7·037	7·095
5	8·516	8·594	8·811	8·997	7·906	7·914	7·937	8·242
6	9·584	9·671	9·913	—	8·940	8·998	9·157	—
7	10·336	10·293	10·174	—	9·651	9·573	9·359	—
8	11·172	11·119	10·971	—	10·440	10·377	10·202	—

TABLE 4

Natural frequency parameters λ for sss moderately thick right triangular plate

	m			
Mode	10	12	Extrapolation	Reference [14]
1	7·509	7·396	7·139	6·948
2	10·929	10·607	9·876	9·651
3	12·187	11·875	11·166	10·875
4	14·841	14·101	12·419	12·300
5	15·676	14·974	13·380	13·210
6	17·107	16·410	14·833	14·559
7	19·364	17·890	14·540	—
8	19·892	18·497	15·326	—

by the proposed method, and Table 3 shows a satisfactory agreement with the previously published results by McGee and Giaimo [13].

Other numerical solutions for the lowest eight values of natural frequency parameter λ of sss moderately thick right triangular plates with uniform thickness were analyzed. The aspect ratio b/a is equal to 1, and the thickness ratio h_0/a is equal to 0·0707. The results for natural frequency are shown in Table 4, and it shows a satisfactory agreement with the previously published results by Kitipornchai *et al.* [14].

8. CONCLUSIONS

Under the concept that a right triangular plate is considered as a kind of rectangular plate with non-uniform thickness, an approximate method was proposed for analyzing the free-vibration problem of various types of right triangular plates by using the Green function of equivalent rectangular plates with non-uniform thickness.

As a result of numerical works, it was shown that the numerical solutions by the proposed method has a good convergence and satisfactory accuracy for various types of thin and moderately thick right triangular plates with uniform and variable thickness.

REFERENCES

1. D. J. GORMAN 1983 *Journal of Sound and Vibration* **89**, 107–118. A highly accurate analytical solution for free vibration analysis of simply supported right triangular plates.
2. D. J. GORMAN 1986 *Journal of Sound and Vibration* **106**, 419–431. Free vibration analysis of right triangular plates with combinations of clamped–simply supported boundary conditions.
3. D. J. GORMAN 1987 *Journal of Sound and Vibration* **112**, 173–176. A modified superposition method for the free vibration analysis of right triangular plates.
4. K. Y. LAM, K. M. LIEW and S. T. CHOW 1990 *International Journal of Mechanical Sciences* **32**, 455–464. Free vibration analysis of isotropic and orthotropic triangular plates.
5. K. M. LIEW 1993 *Journal of Sound and Vibration* **165**, 329–340. On the use of pb-2 Rayleigh–Ritz method for free-flexural vibration of triangular plates with curved internal supports.
6. K. M. LIEW and M. K. LIM 1993 *Journal of Sound and Vibration* **165**, 45–67. Transverse vibration of trapezoidal plates of variable thickness: symmetric trapezoids.
7. H. T. SALIBA 1990 *Journal of Sound and Vibration* **139**, 289–297. Transverse free vibration of simply supported right triangular thin plates: a highly accurate simplified solution.
8. H. T. SALIBA 1995 *Journal of Sound and Vibration* **183**, 765–778. Transverse free vibrations of right triangular thin plates with combinations of clamped and simply supported boundary conditions: a highly accurate simplified solution.
9. C. S. KIM and S. M. DICKINSON 1990 *Journal of Sound and Vibration* **141**, 291–311. The free flexural vibration of right triangular isotropic and orthotropic plates.
10. S. MIRZA and M. BIJLANI 1985 *Computers & Structures* **21**, 1129–1135. Vibration of triangular plates of variable thickness.
11. K. M. LIEW, C. W. LIM and M. K. LIM 1994 *Journal of Sound and Vibration* **177**, 479–501. Transverse vibration of trapezoidal plates of variable thickness: unsymmetric trapezoids.
12. B. SINGH and V. SAXENA 1996 *Journal of Sound and Vibration* **177**, 471–496. Transverse vibration of triangular plates with variable thickness.
13. O. G. MCGEE and G. T. GIAIMO 1992 *Journal of Sound and Vibration* **159**, 279–293. Three-dimensional vibrations of cantilevered right triangular plates.
14. S. KITIPORNCHI, K. M. LIEW, Y. XIANG and C. M. WANG 1993 *International Journal of Mechanical Sciences* **35**, 89–102. Free flexural vibration of triangular Mindlin plates.
15. K. M. LIEW, K. C. HUNG and M. K. LIM 1994 *AIAA Journal* **32**, 2080–2089. Three-dimensional elasticity solutions to vibration of cantilevered skewed trapezoids.
16. T. SAKIYAMA and M. HUANG 1998 *Journal of Sound and Vibration* **216**, 379–397, Free vibration analysis of rectangular plates with variable thickness.

APPENDIX A

$F_{111} = F_{123} = F_{134} = F_{146} = F_{167} = F_{178} = F_{188} = 1, \quad F_{212} = F_{225} = F_{233} = F_{257} = F_{266} = \mu,$

$F_{156} = \nu, \quad F_{247} = \nu\mu, \quad F_{322} = F_{331} = -\mu, \quad F_{344} = F_{355} = -I, \quad F_{363} = -J, \quad F_{372} = -\kappa,$

$F_{377} = 1, \quad F_{381} = -\mu\kappa, \quad F_{386} = \mu, \quad \text{other } F_{1te}, F_{2te}, F_{3te} = 0,$

$I = \mu(1-\nu^2)(h_0/h)^3, \quad J = 2\mu(1+\nu)(h_0/h)^3, \quad \kappa = (1/10)(E/G)(h_0/a)^2(h_0/h).$

APPENDIX B

$A_{p1} = \gamma_{p1}, \quad A_{p2} = 0, \quad A_{p3} = \gamma_{p2}, \quad A_{p4} = \gamma_{p3}, \quad A_{p5} = 0, \quad A_{p6} = \gamma_{p4} + \nu\gamma_{p5}, \quad A_{p7} = \gamma_{p6},$

$A_{p8} = \gamma_{p7}, \quad B_{p1} = 0, \quad B_{p2} = \mu\gamma_{p1}, \quad B_{p3} = \mu\gamma_{p3}, \quad B_{p4} = 0, \quad B_{p5} = \mu\gamma_{p2}, \quad B_{p6} = \mu\gamma_{p6},$

$B_{p7} = \mu(\nu\gamma_{p4} + \gamma_{p5}), \quad B_{p8} = \gamma_{p8}, \quad C_{p1kl} = \mu(\gamma_{p3} + \kappa_{kl}\gamma_{p7}), \quad C_{p2kl} = \mu\gamma_{p2} + \kappa_{kl}\gamma_{p8},$

$C_{p3kl} = J_{kl}\gamma_{p6}, \quad C_{p4kl} = I_{kl}\gamma_{p4}, \quad C_{p5kl} = I_{kl}\gamma_{p5}, \quad C_{p6kl} = -\mu\gamma_{p7}, \quad C_{p7kl} = -\gamma_{p8},$

$C_{p8kl} = 0, \quad [\gamma_{pk}] = [\bar{\gamma}_{pk}]^{-1}, \quad \bar{\gamma}_{11} = \beta_{ii}, \quad \bar{\gamma}_{12} = \mu\beta_{jj}, \quad \bar{\gamma}_{22} = -\mu\beta_{ij}, \quad \bar{\gamma}_{23} = \beta_{ii}, \quad \bar{\gamma}_{25} = \mu\beta_{jj},$

$\bar{\gamma}_{31} = -\mu\beta_{ij}, \quad \bar{\gamma}_{33} = \mu\beta_{jj}, \quad \bar{\gamma}_{34} = \beta_{ii}, \quad \bar{\gamma}_{44} = -I_{ij}\beta_{ij}, \quad \bar{\gamma}_{46} = \beta_{ii}, \quad \bar{\gamma}_{47} = \mu\nu\beta_{jj}, \quad \bar{\gamma}_{55} = -I_{ij}\beta_{ij},$

$\bar{\gamma}_{56} = \nu\beta_{ii}, \quad \bar{\gamma}_{57} = \mu\beta_{jj}, \quad \bar{\gamma}_{63} = -J_{ij}\beta_{ij}, \quad \bar{\gamma}_{66} = \mu\beta_{jj}, \quad \bar{\gamma}_{67} = \beta_{ii}, \quad \bar{\gamma}_{71} = -\mu\kappa_{ij}\beta_{ij}, \quad \bar{\gamma}_{76} = \mu\beta_{ij},$

$\bar{\gamma}_{78} = \beta_{ii}, \quad \bar{\gamma}_{82} = -\kappa_{ij}\beta_{ij}, \quad \bar{\gamma}_{87} = \beta_{ij}, \quad \bar{\gamma}_{88} = \beta_{jj}, \quad \textit{other } \bar{\gamma}_{pk} = 0, \quad \beta_{ij} = \beta_{ii}\beta_{jj}.$

APPENDIX C

$a_{11i0i1} = a_{13i0i2} = a_{14i0i3} = a_{16i0i4} = a_{17i0i5} = a_{18i0i6} = 1, \qquad a_{15i0i3} = \nu,$

$a_{220jj1} = a_{230jj2} = a_{250jj3} = a_{260jj4} = a_{270jj5} = a_{280jj6} = 1, \qquad a_{240jj3} = \nu, \quad a_{230002} = 0,$

$$a_{hpijuv} = \sum_{e=1}^{8} \left\{ \begin{array}{l} \displaystyle\sum_{k=0}^{i} \beta_{ik} A_{pe} [a_{hek0uv} - a_{hekjuv}(1-\delta_{ki})] + \sum_{l=0}^{i} \beta_{jl} B_{pe} [a_{he0luv} - a_{heiluv}(1-\delta_{lj})] \\ \displaystyle + \sum_{k=0}^{i} \sum_{l=0}^{j} \beta_{ik}\beta_{jl} C_{pekl} a_{hekluv}(1-\delta_{ki}\delta_{lj}), \end{array} \right\}$$

where $h = 1, 2$, $p = 1, 2, \ldots, 8$, $i = 1, 2, \ldots, m$, $j = 1, 2, \ldots, n$, $v = 1, 2, \ldots, 6$, $u = 0, 1, \ldots, i$ $(h = 1)$, $0, 1, \ldots, j$ $(h = 2)$,

$$q_{fpijcd} = \sum_{e=1}^{8} \left\{ \begin{array}{l} \displaystyle\sum_{k=0}^{i} \beta_{ik} A_{pe} [q_{fek0cd} - q_{fekjcd}(1-\delta_{ki})] + \sum_{l=0}^{i} \beta_{jl} B_{pe} [q_{fe0lcd} - q_{feilcd}(1-\delta_{lj})] \\ \displaystyle + \sum_{k=0}^{i} \sum_{l=0}^{j} \beta_{ik}\beta_{jl} C_{pekl} q_{feklcd}(1-\delta_{ki}\delta_{lj}) \end{array} \right\}$$

$$- \gamma_{pf} \sum_{k=0}^{i} \sum_{l=0}^{j} u_{ik} u_{jl} \bar{u}_{fkl},$$

where

$$\bar{u}_{fkl} = \begin{cases} 0 & \text{non-existing point support,} \\ 1 & \text{existing point support,} \end{cases}$$

$$\bar{q}_{pij} = \sum_{e=1}^{8} \left\{ \begin{array}{l} \displaystyle\sum_{k=0}^{i} \beta_{ik} A_{pe} [\bar{q}_{ek0} - \bar{q}_{ekj}(1 - \delta_{ki})] + \sum_{l=0}^{i} \beta_{jl} B_{pe} [\bar{q}_{e0l} - \bar{q}_{eil}(1 - \delta_{lj})] \\ \\ \displaystyle + \sum_{k=0}^{i} \sum_{l=0}^{j} \beta_{ik} \beta_{jl} C_{pekl} \bar{q}_{ekl} (1 - \delta_{ki} \delta_{lj}) \end{array} \right\}$$

$$- \gamma_{p1} u_{iq} u_{jr}.$$